# Gray solitary-wave solutions in nonlinear negative-index materials

Penggang Li,[1] Rongcao Yang,[1,2,*] and Zhiyong Xu[2]
[1]*College of Physics & Electronics Engineering, Shanxi University, Taiyuan 030006, China*
[2]*Nonlinear Physics Center, Research School of Physics and Engineering, Australian National University, Canberra, Australian Capital Territory 0200, Australia*

(Received 29 October 2009; revised manuscript received 30 July 2010; published 15 October 2010)

We predict the existence of gray (dark) solitary waves in negative-index materials on the basis of a derived higher-order nonlinear Schrödinger equation. The conditions for the formation of three cases of gray solitary waves and exact analytical expressions are presented. Furthermore, we investigate the properties of these gray solitary waves in negative-index materials. The results show that the higher-order linear and nonlinear effects play a crucial role for the formation and properties of the second and third cases of gray solitary waves.

DOI: 10.1103/PhysRevE.82.046603 PACS number(s): 05.45.Yv, 42.65.Tg, 42.65.Sf, 41.20.Jb

## I. INTRODUCTION

Since the experimental confirmation of Veselago's prediction of negative-index materials (NIMs) with simultaneously negative electric and magnetic responses [1,2], NIMs have attracted a lot of interest due to the remarkable property of having an antiparallel phase velocity and Poynting vector [3–9]. Recently, nonlinear effects in NIMs have been extensively studied, including second-harmonic generation [10], parametric amplification [11], modulation instability [12], and soliton propagation [13–21]. It is well known that nonlinear NIMs not only possess dispersive magnetic permeability, which leads to the difference between the dynamic models for the envelopes of the electromagnetic wave in NIMs and in ordinary materials, but also support rich localized modes [13–21]. These localized modes in nonlinear NIMs can take the forms of gap solitons [13], spatial solitons [14], spatiotemporal solitons [15,16], and temporal solitons [17–21]. In particular, small-amplitude dark and bright solitons on the background of a continuous wave in NIMs have been obtained by employing small-amplitude soliton approximation method [20]. Dark solitons and their interactions in metamaterials have been studied by using a Korteweg-de Vries description [21]. To best of our knowledge, the study on gray (dark) solitons in NIMs still remains new.

The properties of dark solitons in ordinary materials have been well investigated both in theories and experiments [22–28]. Dark solitons are generally considered to be less desirable for applications in high-speed communication systems because of their higher average power, but they have better stability against material loss and background noise than bright solitons do [24]. Moreover, the time jitter in dark solitons is much lower, and the interaction between neighboring dark solitons is much less than that for their bright counterparts [25–27]. Since there are striking differences between ordinary materials and NIMs, in which the former have a constant permeability and positive refraction while the latter have a dispersive permeability and negative refraction, it is necessary to investigate the properties of dark solitons in NIMs. In this paper, motivated by the work of Scalora *et al.* [18], we derive an extended nonlinear Schrödinger (NLS) equation including third-order dispersion (TOD) and second-order nonlinear dispersion effects, which describes the propagation of few-cycle electromagnetic pulses in nonlinear NIMs. Furthermore, we present three cases of exact gray (dark) solitary-wave solutions for this equation by ansatz method and investigate the formation conditions and properties of these solutions in detail.

## II. THEORETICAL MODELS

NIMs are composed of a regular array of unit cells whose size is usually much smaller than the wavelengths of propagating electromagnetic waves. Therefore, NIMs may be considered as continuous and homogeneous according to effective-medium theory and may be described by effective $\varepsilon(\omega)$ and $\mu(\omega)$ [17,18]. Let us consider the propagation of electromagnetic wave in an isotropic and homogeneous NIM, whose $\varepsilon(\omega)$ and $\mu(\omega)$ can be expanded in Taylor series [18],

$$\omega\varepsilon(\omega) = \sum_{n=0}^{\infty} \left\{ \frac{\partial^n [\omega\varepsilon(\omega)]}{\partial\omega^n}\bigg|_{\omega=\omega_0} \frac{(\omega-\omega_0)^n}{n!} \right\}, \tag{1a}$$

$$\omega\mu(\omega) = \sum_{n=0}^{\infty} \left\{ \frac{\partial^n [\omega\mu(\omega)]}{\partial\omega^n}\bigg|_{\omega=\omega_0} \frac{(\omega-\omega_0)^n}{n!} \right\}, \tag{1b}$$

where $\omega_0$ is the carrier frequency of the incident electromagnetic wave. Substituting Eqs. (1) into Maxwell's equations, one can obtain a system of coupled nonlinear Schrödinger equations, [18]

$$\frac{\partial E_x(z,t)}{\partial z} = \frac{i}{c} e^{ikz-i\omega_0 t} \sum_{n=0}^{\infty} \left\{ i^n \frac{\partial^n(\omega\mu)}{\partial\omega^n}\bigg|_{\omega=\omega_0} \frac{1}{n!} \frac{\partial^n H(z,t)}{\partial t^n} \right\}, \tag{2a}$$

*Corresponding author; sxdxyrc@sxu.edu.cn

 

$$\frac{\partial H_y(z,t)}{\partial z} = \frac{i}{c} e^{ikz - i\omega_0 t} \sum_{n=0}^{\infty} \left\{ i^n \frac{\partial^n(\omega\varepsilon)}{\partial \omega^n}\bigg|_{\omega=\omega_0} \frac{1}{n!} \frac{\partial^n E(z,t)}{\partial t^n} \right\} - \frac{1}{c}\frac{\partial}{\partial t} P_{nl}(z,t), \tag{2b}$$

where $E_x(z,t)=E(z,t)e^{i(kz-\omega t)}$ and $H_y(z,t)=H(z,t)e^{i(kz-\omega t)}$. Here, $E(z,t)$ and $H(z,t)$ are the envelopes of the electric and magnetic fields, respectively. $P_{nl}=\chi^{(3)}|E|^2E+\chi^{(5)}|E|^4E+\cdots$ is the nonlinear polarization and $\chi^{(n)}$ is the $n$-order nonlinear susceptibility. It should be noticed that, in typical nonlinear NIMs, there exists significant magnetic nonlinearity [5]. However, the symmetry of Eqs. (2a) and (2b) for electric field $E$ and magnetic field $H$ suggests that nonlinear magnetization produces qualitatively similar effects [18], leading to similar propagation equation for the magnetic field. Therefore, here we consider the wave propagation in the case of nonlinear polarization. Equations (2) are very general because they include any desired order of dispersion and susceptibility. In order to investigate the higher-order linear and nonlinear effects on the propagation of ultrashort electromagnetic waves, here we retain linear derivatives up to the third-order and neglect nonlinear third-order temporal derivatives; thus, Eq. (2) can be simplified as

$$\alpha\frac{\partial E}{\partial \tau} + i\frac{\alpha'}{4\pi}\frac{\partial^2 E}{\partial \tau^2} - \frac{1}{6}\frac{\alpha''}{4\pi^2}\frac{\partial^3 E}{\partial \tau^3} = i\beta\varepsilon E - i\beta n H - \frac{\partial H}{\partial \xi} + i\beta\chi^{(3)} \times |E|^2E - \chi^{(3)}\frac{\partial}{\partial \tau}(|E|^2E), \tag{3a}$$

$$\gamma\frac{\partial H}{\partial \tau} + i\frac{\gamma'}{4\pi}\frac{\partial^2 H}{\partial \tau^2} - \frac{1}{6}\frac{\gamma''}{4\pi^2}\frac{\partial^3 H}{\partial \tau^3} = i\beta\mu H - i\beta n E - \frac{\partial E}{\partial \xi}, \tag{3b}$$

where $\alpha=\partial[\tilde{\omega}\varepsilon(\tilde{\omega})]/\partial\tilde{\omega}$, $\alpha'=\partial^2[\tilde{\omega}\varepsilon(\tilde{\omega})]/\partial^2\tilde{\omega}$, $\alpha''=\partial^3[\tilde{\omega}\varepsilon(\tilde{\omega})]/\partial^3\tilde{\omega}$, $\gamma=\partial[\tilde{\omega}\mu(\tilde{\omega})]/\partial\tilde{\omega}$, $\gamma'=\partial^2[\tilde{\omega}\mu(\tilde{\omega})]/\partial^2\tilde{\omega}$, $\gamma''=\partial^3[\tilde{\omega}\mu(\tilde{\omega})]/\partial^3\tilde{\omega}$, $\xi=z/\lambda_p$, $\tau=ct/\lambda_p$, $\beta=2\pi\tilde{\omega}=2\pi\omega/\omega_p$, and $n=\sqrt{\varepsilon\mu}=n(\tilde{\omega})$. Here, $\omega_p$ is the electric plasma frequency and $\lambda_p$ is the corresponding wavelength, which is determined by the structure of NIMs. Combining Eqs. (3a) and (3b) and eliminating magnetic fields, we have

$$\begin{aligned}\frac{\partial E}{\partial \xi} + \frac{(\varepsilon\gamma+\mu\alpha)}{2n}\frac{\partial E}{\partial \tau} &= \frac{i}{2\beta n}\left(\frac{\partial^2 E}{\partial \xi^2} - \alpha\gamma\frac{\partial^2 E}{\partial \tau^2}\right) + \frac{1}{8\pi\beta n}\left(\alpha\gamma' + \gamma\alpha' + \beta\frac{\varepsilon\gamma''+\mu\alpha''}{6\pi}\right)\frac{\partial^3 E}{\partial \tau^3} \\ &+ \frac{i\beta\mu\chi^{(3)}}{2n}|E|^2E - \frac{(\gamma+\mu)\chi^{(3)}}{2n}\frac{\partial}{\partial \tau}(|E|^2E) \\ &- \frac{i(\varepsilon\gamma'+\mu\alpha')}{8\pi n}\frac{\partial^2 E}{\partial \tau^2} - \frac{i\chi^{(3)}}{2\beta n}\left(\gamma+\frac{\beta\gamma'}{4\pi}\right)\frac{\partial^2}{\partial \tau^2}(|E|^2E).\end{aligned} \tag{4}$$

From Eq. (4), one can see that the wave propagates at a group velocity $V_g=2n/(\varepsilon\gamma+\mu\alpha)$ (in units of $c$). For relatively transparent NIMs [18,29], $\alpha>0$, $\gamma>0$, and $n<0$; therefore, $V_g$ is always positive. In addition, it should be noticed that Eq. (4) is not suitable for the case of $n\to 0$. In this case one should solve Eqs. (3) directly. Introducing a retarded coordinate $\partial/\partial\zeta=\partial/\partial\xi+(1/V_g)(\partial/\partial\tau)$, Eq. (4) can be written as

$$\begin{aligned}\frac{\partial E}{\partial \zeta} &= \frac{i}{2\beta n}\left(\frac{1}{V_g^2} - \alpha\gamma - \beta\frac{\varepsilon\gamma'+\mu\alpha'}{4\pi}\right)\frac{\partial^2 E}{\partial \tau^2} \\ &+ \frac{1}{8\pi\beta n}\left(\alpha\gamma' + \gamma\alpha' + \beta\frac{\varepsilon\gamma''+\mu\alpha''}{6\pi}\right)\frac{\partial^3 E}{\partial \tau^3} \\ &+ \frac{i\beta\mu\chi^{(3)}}{2n}|E|^2E + \frac{i}{2\beta n}\left(\frac{\partial^2 E}{\partial \zeta^2} - \frac{2}{V_g}\frac{\partial^2 E}{\partial \zeta\,\partial \tau}\right) \\ &- \chi^{(3)}\frac{\gamma+\mu}{2n}\frac{\partial}{\partial \tau}(|E|^2E) - \frac{i\chi^{(3)}}{2\beta n}\left(\gamma+\frac{\beta\gamma'}{4\pi}\right)\frac{\partial^2}{\partial \tau^2}(|E|^2E).\end{aligned} \tag{5}$$

Differentiating Eq. (5) with respect to $\zeta$ and $\tau$, respectively, and neglecting the fourth-order linear derivative and third-order nonlinear temporal derivative [30], we can estimate $\partial^2E/\partial\zeta^2$ and $\partial^2E/\partial\zeta\,\partial\tau$ in the following approximations:

$$\frac{\partial^2 E}{\partial \zeta^2} \approx \frac{i\beta\mu\chi^{(3)}}{2n}\frac{\partial}{\partial \zeta}(|E|^2E) - \frac{\beta\mu\chi^{(3)}k_2}{4n}\frac{\partial^2}{\partial \tau^2}(|E|^2E), \tag{6a}$$

$$\begin{aligned}\frac{\partial^2 E}{\partial \zeta\,\partial \tau} &\approx \frac{i\beta\mu\chi^{(3)}}{2n}\frac{\partial}{\partial \tau}(|E|^2E) \\ &+ \frac{\chi^{(3)}}{2n}\left[\frac{\mu}{nV_g} - (\gamma+\mu)\right]\frac{\partial^2}{\partial \tau^2}(|E|^2E) + \frac{ik_2}{2}\frac{\partial^3 E}{\partial \tau^3},\end{aligned} \tag{6b}$$

where $k_2=(\partial/\partial\omega)(1/V_g)=(1/\beta n)[1/V_g^2-\alpha\gamma-\beta(\varepsilon\gamma'+\mu\alpha')/4\pi]$ is the group velocity dispersion (GVD) coefficient. Substituting Eqs. (6) into Eq. (5), we can obtain a generalized higher-order NLS equation,

$$\frac{\partial E}{\partial \zeta} = \frac{ik_2}{2}\frac{\partial^2 E}{\partial \tau^2} + k_3\frac{\partial^3 E}{\partial \tau^3} + ip_3|E|^2E - ip_5|E|^4E + s_1\frac{\partial}{\partial \tau}(|E|^2E) - is_2\frac{\partial^2}{\partial \tau^2}(|E|^2E), \tag{7}$$

where $k_3=(1/2\beta n)[(k_2/V_g)+\beta(\varepsilon\gamma''+\mu\alpha'')/24\pi^2+(\alpha\gamma'+\gamma\alpha')/4\pi]$ is the TOD coefficient. $p_3=\beta\mu\chi^{(3)}/(2n)$ and $p_5=\beta\mu^2(\chi^{(3)})^2/(8n^3)$ describe $\chi^{(3)}$ and pseudo-$\chi^{(5)}$ nonlinearities, respectively. $s_1=(\chi^{(3)}/2n)[(\mu/V_gn)-(\gamma+\mu)]$ and $s_2=(\mu\chi^{(3)}/2n)[(k_2/4n)+(\gamma/\mu\beta)+(\gamma'/4\pi\mu)]$ are related to the self-steepening and second-order nonlinear dispersion effects. In Eq. (7), all linear and nonlinear dispersive coefficients are related to the dispersive permeability $\mu$. Comparing Eq. (7) for the propagation of electromagnetic waves in NIMs with that in ordinary materials [27], the main difference is additional second-order nonlinear dispersion and pseudo-$\chi^{(5)}$ nonlinearity that come from the combination of $\chi^{(3)}$ and $\mu$. These additional terms become significant in the formation of solitons, as will be shown in subsequent sec-

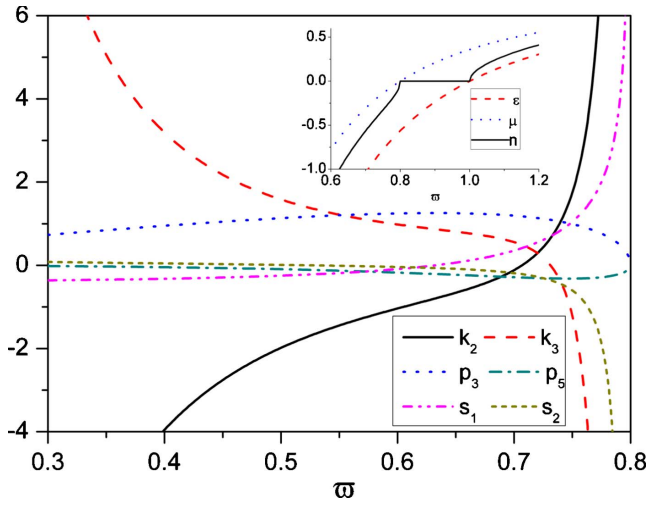


FIG. 1. (Color online) Curves of $k_2$, $k_3$, $p_3$, $p_5$, $s_1$, and $s_2$ versus $\tilde{\omega}$ in focusing NIMs for $\omega_m/\omega_p=0.8$. Here, $p_3$, $s_1$, and $s_2$ are plotted in units of $\chi^{(3)}$, and $p_5$ in units of $(\chi^{(3)})^2$. Inset: curves of $\varepsilon$, $\mu$, and $n$ versus $\tilde{\omega}$ for $\omega_m/\omega_p=0.8$.

tions. When neglecting the TOD and second-order nonlinear dispersion, i.e., $k_3=s_2=0$, Eq. (7) is reduced to Eq. (12) in Ref. [18], which paved the way for realizing a wide class of solitary waves in NIMs. When all linear and nonlinear higher-order effects are considered, Eq. (7) is similar to the model that was used to describe the propagation of few-cycle pulses [12,20]. However, it should be noted that all coefficients in Eq. (7) are directly expressed by material $\varepsilon$ and $\mu$. Therefore, model (7) may be conveniently used to investigate the influence of material parameters on the propagation of ultrashort pulses. Here, we adopt a lossy Drude mode described by [29] $\varepsilon(\tilde{\omega})=1-[1/\tilde{\omega}(\tilde{\omega}+i\tilde{\gamma}_e)]$, $\mu(\tilde{\omega})=1-[(\omega_m^2/\omega_p^2)/\tilde{\omega}(\tilde{\omega}+i\tilde{\gamma}_m)]$, where $\tilde{\omega}=\omega/\omega_p$, $\tilde{\gamma}_e=\gamma_e/\omega_p$, and $\tilde{\gamma}_m=\gamma_m/\omega_p$ are the respective normalized frequency and electric and magnetic loss terms, and $\omega_p$ and $\omega_m$ are the respective electric and magnetic plasma frequencies. We choose the typical value $\tilde{\gamma}_e\approx\tilde{\gamma}_m\approx4.5\times10^{-4}$, which results in very low absorption [12,18,31]. In general, the losses of NIMs originate from the intrinsic absorption, resonant nature of magnetic response, etc., so they are inevitable [11,32–34]. Nevertheless, several approaches have been proposed to reduce or compensate the losses in NIMs including novel fabrication methods [32,33] and optical parametric amplification [11]. Therefore, for simplicity we neglect the losses in the following discussion. Figure 1 shows the dependences of material and model parameters on $\tilde{\omega}$ at $\omega_m/\omega_p=0.8$ for focusing NIMs. From the inset one can see that for $\omega_m/\omega_p=0.8$, $\varepsilon$, $\mu$, and $n$ are all negative when $\tilde{\omega}<0.8$. The effects of pseudo-$\chi^{(5)}$ and $\chi^{(3)}$ nonlinearities mutually enhance for focusing NIMs due to $p_3>0$ and $p_5<0$ [the signs of $p_3$ and $p_5$ are opposite in Eq. (7)]. It is well known that the size and element of NIMs may influence the electric and magnetic plasma frequencies which result in the change of the model parameters in Eq. (7). Thus, GVD, TOD, self-steepening, and second-order nonlinear dispersion can be altered by engineering the structure of NIMs. This property may provide more possibilities for the formation of solitons in NIMs. It should be pointed out that all parameters are not isolated, but comply with the relation presented in Fig. 1 at a given plasma frequency. In the following, we will investigate the formations and properties of gray solitary waves and take values of the model parameters based on the relation in Fig. 1.

## III. EXACT GRAY SOLITARY-WAVE SOLUTIONS

To search for gray solitary-wave solutions of Eq. (7), we take an ansatz as follows:

$$E(\zeta,\tau)=\{\lambda+i\rho\tanh[\eta(\tau-\chi\zeta)]\}\exp[i(k\zeta-\Omega\tau)], \quad (8)$$

whose intensity is $|E(\zeta,\tau)|^2=\lambda^2+\rho^2\tanh^2[\eta(\tau-\chi\zeta)]$. It is clear to see that Eq. (8) denotes a gray (dark) solitary wave when $\lambda\neq0$ ($\lambda=0$), where $\lambda$ and $\rho$ are, respectively, related to the amplitude and the dip depth of the gray solitary wave, and $\eta$, $\chi$, $k$, and $\Omega$ are the respective real parameters describing inverse pulse width, inverse group velocity, wave number, and frequency shift. Substituting Eq. (8) into Eq. (7) and setting the coefficients of independent terms equal to zero, we can obtain six compatible equations:

$$\begin{aligned}&2(k\lambda-\eta\rho\chi)-k_2\Omega(2\eta\rho-k_2\lambda\Omega)-2\lambda^3(p_3-p_5\lambda^2)\\&-2\lambda^2s_1(\eta\rho-2\lambda\Omega)+2k_3(2\eta^3\rho+3\eta\rho\Omega^2-\lambda\Omega^3)\\&+2\lambda s_2(2\rho^2\eta^2+2\eta\rho\Omega\lambda-\lambda^2\Omega^2)=0,\end{aligned} \quad (9a)$$

$$\begin{aligned}&2k+2\lambda s_1(2\eta\rho+\lambda\Omega)+k_2(2\eta^2+\Omega^2)-2\lambda^2(p_3-p_5\lambda^2)\\&-2k_3\Omega(6\eta^2+\Omega^2)\\&-2s_2(2\eta^2\lambda-6\eta^2\rho^2+4\eta\rho\lambda\Omega+\lambda^2\Omega^2)=0,\end{aligned} \quad (9b)$$

$$\begin{aligned}&\eta(\chi+k_2\Omega-8k_3\eta^2-3k_3\Omega^2)+s_1(\eta\lambda^2-3\eta\rho^2+\lambda\rho\Omega)\\&-\lambda\rho(p_3+2p_5\lambda^2)\\&-s_2(8\eta^2\rho\lambda+2\eta\lambda^2\Omega-6\eta\rho^2\Omega+\lambda\rho\Omega^2)=0,\end{aligned} \quad (9c)$$

$$\begin{aligned}&\eta^2(k_2-6k_3\Omega-2\lambda^2s_2+18\rho^2s_2)-\rho\Omega s_2(4\eta\lambda-\rho\Omega)\\&+\rho(\rho p_3-2\lambda^2\rho p_5+2\eta\lambda s_1-\rho\Omega s_1)=0,\end{aligned} \quad (9d)$$

$$6k_3\eta^3+p_5\lambda\rho^3+3\eta\rho^2s_1+6\eta\rho(\eta\lambda-\rho\Omega)s_2=0, \quad (9e)$$

$$p_5\rho^2+12\eta^2s_2=0. \quad (9f)$$

Solving Eqs. (9a)–(9f), we find that there exist three cases of exact gray (dark) solitary-wave solutions for Eq. (7).

(i) When all higher-order effects are neglected, i.e., $k_3=p_5=s_1=s_2=0$, Eq. (7) is reduced to a standard NLS equation which admits the following gray solitary-wave solution:

$$\begin{aligned}E(\zeta,\tau)=&\left(\lambda+i\eta\sqrt{-\frac{k_2}{p_3}}\right.\\&\times\tanh\left\{\eta\left[\tau+\left(\lambda k_2\sqrt{-\frac{p_3}{k_2}}+k_2\Omega\right)\zeta\right]\right\}\Bigg)\\&\times\exp\left\{i\left[\left(\lambda^2p_3-\eta^2k_2-\frac{k_2\Omega^2}{2}\right)\zeta-\Omega\tau\right]\right\},\end{aligned} \quad (10)$$

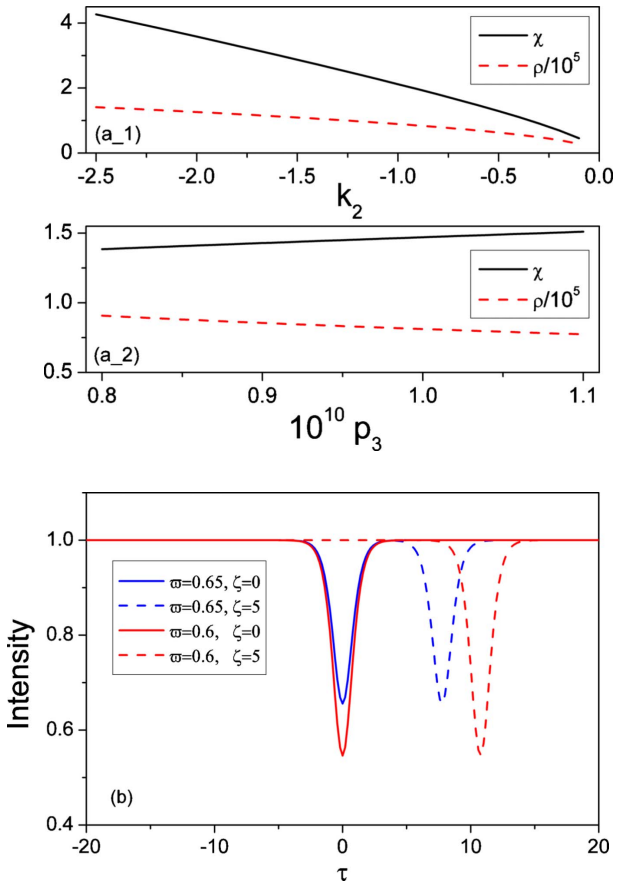


FIG. 2. (Color online) (a) The influences of model parameters $k_2$ and $p_3$ on $\chi$ and $\rho$ of gray solitary wave (10) for $\omega_m/\omega_p=0.8$, $\tilde{\omega}=0.65$; (b) the distributions of the gray solitary wave (10) for $\omega_m/\omega_p=0.8$ when $\tilde{\omega}=0.65$, corresponding to $k_2=-0.6589$, $p_3=1.2532\times10^{-10}$, and $\tilde{\omega}=0.6$, corresponding to $k_2=-1.0372$, $p_3=1.2468\times10^{-10}$. Here, soliton intensities are normalized by $|E|^2\to|E|^2/(\rho^2+\lambda^2)$ and $\eta=1$, $\Omega=1$, and $\lambda=10^5$.

where $\eta$, $\lambda$, and $\Omega$ are arbitrary constants. It is noted that for this special case without higher-order effects, the gray solitary wave (10) is in agreement with solution (12) of Ref. [35], which was obtained in nonlinear magnetic metamaterials. From expression (10), we can see that the GVD and nonlinearity must satisfy the condition $k_2p_3<0$, which implies that the gray solitary wave can exist in abnormal (normal) dispersion for self-focusing (-defocusing) nonlinearity. This is different from that in ordinary materials. Moreover, the dip depth related to $\eta\sqrt{-k_2/p_3}$ and its velocity $\lambda k_2\sqrt{-p_3/k_2}+k_2\Omega$ depend on $k_2$ and $p_3$; the dependent relationships are shown in Fig. 2(a). Figure 2(b) presents the distributions of the gray solitary wave (10) with different dip depths and velocities under different dispersions and nonlinearities.

(ii) When pseudo-$\chi^{(5)}$ nonlinearity and the second-order nonlinear dispersion are neglected, i.e., $s_2=p_5=0$, Eq. (7) has a gray solitary-wave solution with the following parameters:

$$\eta^2=-\frac{\rho^2 s_1}{2k_3}, \tag{11a}$$

$$\Omega=\frac{k_2}{4k_3}-\frac{p_3}{2s_1}-\frac{\lambda\eta}{\rho}, \tag{11b}$$

$$\chi=-\frac{k_2^2}{16k_3}+\frac{3k_3p_3^2}{4s_1^2}-\frac{k_2p_3}{4s_1}-\left(\frac{3\lambda^2}{2}+\rho^2\right)s_1, \tag{11c}$$

$$k=-\frac{k_2^3}{64k_3^2}-\frac{k_3p_3^3}{8s_1^3}+\frac{k_2p_3^2}{16s_1^2}+\frac{k_2^2p_3}{32k_3s_1}-\frac{3k_2\lambda^2s_1+2k_2\rho^2s_1}{8k_3}+\frac{\lambda k_2^2\eta}{16\rho k_3}-\frac{3\lambda k_3p_3^2\eta}{4\rho s_1^2}+\frac{\lambda k_2p_3\eta}{4\rho s_1}+\frac{3\lambda^3s_1\eta}{2\rho}+\frac{9\lambda^2p_3+6\rho^2p_3}{4}+\lambda\eta\rho s_1, \tag{11d}$$

where $\lambda$ is a free parameter. Equation (11a) implies that the TOD $k_3$ and self-steepening $s_1$ must satisfy $s_1k_3<0$, and the width $\eta$ and the dip depth $\rho$ are related to each other, which just reflects the intrinsic characteristics of solitons. Other soliton parameters $\chi$, $k$, $\eta$, and $\Omega$ are also related to the TOD $k_3$ and the self-steepening $s_1$ [see Eqs. (11b)–(11d)]. Figures 3(a) and 3(b) present the dependences of the velocity $\chi$, wave number $k$, width $\eta$, and frequency shift $\Omega$ on the TOD $k_3$ and the self-steepening $s_1$, respectively. It is clear that the influence of $k_3$ and $s_1$ on $\chi$ and $k$ is much stronger than on $\Omega$ and $\eta$. This is the reason why in Fig. 3(c), the width of the gray solitary wave (11) hardly changes, while its velocity is distinctly different under different $k_3$'s and $s_1$'s. These results show that the TOD and the self-steepening effects not only influence the existence condition of this gray solitary wave (11), but also dominate its propagation properties in NIMs. Figure 3(d) shows the evolution of this gray solitary wave (11) in NIMs for $\omega_m/\omega_p=0.9$ and $\tilde{\omega}=0.6$. The inset displays the comparison of exact solution with the numerical simulations. As shown in the inset, our analytical results are in good agreement with the numerical simulations.

(iii) When all higher-order effects in Eq. (7) are considered, i.e., $s_2\neq0, p_5\neq0, s_1\neq0, k_3\neq0$, the gray solitary wave possesses the following parameters:

$$\eta^2=-\frac{p_5\rho^2}{12s_2}, \tag{12a}$$

$$\Omega=-\frac{\lambda\eta}{\rho}-\frac{k_3p_5}{12s_2^2}+\frac{s_1}{2s_2}, \tag{12b}$$

$$\chi=\frac{\eta\lambda(k_2+23\lambda^2s_2)}{\rho}+\frac{3\eta\lambda(s_1^2-4p_3s_2)}{\rho p_5}+\frac{k_3^2p_5^2}{48s_2^4}-\frac{k_3^2p_5s_1}{4s_2^3}+\frac{k_2k_3p_5-9k_3s_1^2}{12s_2^2}+\frac{5\lambda k_3^2p_5\eta}{12\rho s_2^2}-\frac{(3\lambda^2+2\rho^2)k_3p_5+6k_2s_1}{12s_2}-\frac{3\lambda k_3s_1\eta}{\rho s_2}+14\lambda\rho\eta s_2, \tag{12c}$$

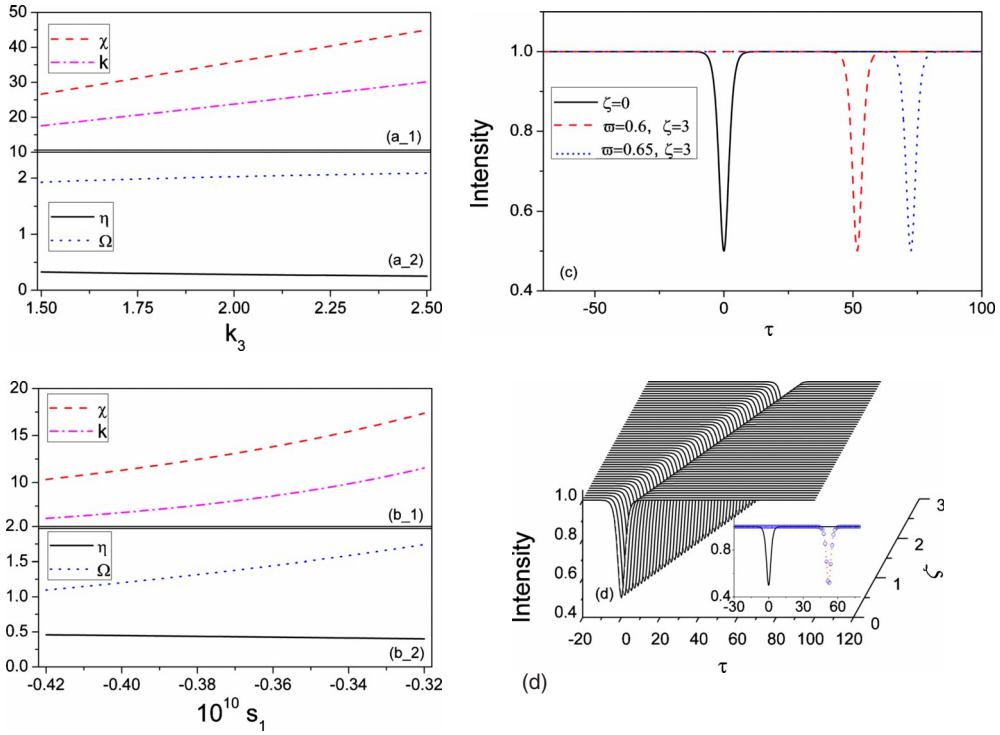


FIG. 3. (Color online) The influences of the higher-order effects (a) $k_3$ and (b) $s_1$ on $\chi$, $k$, $\eta$, and $\Omega$ of the gray solitary wave (11) for $\omega_m/\omega_p=0.9$, $\tilde{\omega}=0.6$; (c) the distributions of the gray solitary wave (11) for $\omega_m/\omega_p=0.9$ when $\tilde{\omega}=0.65$, corresponding to $k_2=-1.0125$, $p_3=1.6727\times10^{-10}$, $k_3=0.8358$, and $s_1=-0.2626\times10^{-10}$, and $\tilde{\omega}=0.6$, corresponding to $k_2=-1.3073$, $p_3=1.5806\times10^{-10}$, $k_3=0.9996$, and $s_1=-0.3197\times10^{-10}$. (d) The evolution of the gray solitary wave (11) for $\omega_m/\omega_p=0.9$, $\tilde{\omega}=0.6$. The inset shows the comparison of the analytical solution (11) (circle) with numerical simulation (dotted line) and initial pulse (solid line). Here, $\lambda=10^5$, $\rho=10^5$, and soliton intensities are normalized as in Fig. 2.

$$k=-\frac{k_3^4p_5^3}{1728s_2^6}+\frac{k_3^3p_5^2s_1}{96s_2^5}-\frac{k_3^2p_5(k_2p_5+18s_1^2)}{288s_2^4}-\frac{\eta\lambda k_3^3p_5^2}{48\rho s_2^4}+\frac{\lambda k_3^2p_5s_1\eta}{4\rho s_2^3}+\frac{k_3[(2\lambda^2+3\rho^2)k_3p_5^2+3k_2p_5s_1+9s_1^3]}{72s_2^3}-\frac{\eta\lambda k_3(k_2p_5+9s_1^2)}{12\rho s_2^2}-\frac{s_1(k_2p_5\lambda^2+2k_3p_5\rho^2+k_2s_1)}{8s_2^2}+\frac{k_2p_5(\lambda^2+2\rho^2)+2\lambda(2\eta\rho k_3p_5-3\lambda s_1^2)}{24s_2}+\frac{\lambda\eta(\lambda^2k_3p_5+2k_2s_1)}{4\rho s_2}+\frac{12\lambda^2p_3-(13\lambda^4+2\lambda^2\rho^2+6\rho^4)p_5}{12}, \tag{12d}$$

$$3\lambda^2+2\rho^2=\frac{-5k_3^2p_5^2+36k_3p_5s_1s_2-12k_2p_5s_2^2-36s_1^2s_2^2-144p_3s_2^3}{108p_5s_2^3}. \tag{12e}$$

Obviously, $\eta$ and $\rho$ are related by Eq. (12a) and $\lambda$ and $\rho$ are related by Eq. (12e), so there is one free parameter among them. Meanwhile, Eq. (12a) requires pseudo-$\chi^{(5)}$ nonlinearity and second-order nonlinear dispersion must satisfy $s_2p_5<0$, and Eq. (12e) requires $-5k_3^2p_5^2+36k_3p_5s_1s_2-12k_2p_5s_2^2-36s_1^2s_2^2+144p_3s_2^3<0$. These conditions mean that the formation of this gray solitary wave (12) strongly depends on pseudo-$\chi^{(5)}$ nonlinearity $p_5$ and second-order nonlinear dispersion $s_2$. It is noted that the formation conditions are relatively strict. According to the relation of model parameters shown in Fig. 1, we find that this gray solitary wave (12) may exist in NIMs. For example, for $\omega_m/\omega_p=0.9$ and $\tilde{\omega}=0.42$, corresponding to $k_2=-3.8616$, $k_3=2.9176$, $p_3=1.1573\times10^{-10}$, $p_5=-0.061\,968\times10^{-20}$, $s_1=-0.410\,38\times10^{-10}$, and $s_2=0.0571\,18\times10^{-10}$, the evolution of this gray solitary wave (12) in NIMs is shown in Fig. 4(a) and the corresponding numerical verification is shown in the inset. It is clear that the analytical solution well coincides in the numerical simulation. Furthermore, we investigate the influence of the higher-order effects such as the TOD $k_3$, self-steepening $s_1$, pseudo-$\chi^{(5)}$ $p_5$, and second-order nonlinear dispersion $s_2$ on the width $\eta$, dip depth $\rho$, velocity $\chi$, frequency shift $\Omega$, and wave number $k$ of the solitary wave (12), as shown in Figs. 4(b)–4(e). It should be pointed out that in order to ensure the model parameters located in the negative-index region, we take the values of these higher-order terms according to Fig. 1. Similar to case (ii), these higher-order effects influence much more the velocity $\chi$ and wave number $k$ than the width $\eta$, dip depth $\rho$, and frequency shift $\Omega$. Figure 4(f) presents the curves of the output pulses at $\zeta=0.2$ at $\tilde{\omega}=0.5$ and 0.45 for $\omega_m/\omega_p=0.9$. It can be seen from Fig. 4(f) that under the different balances of param-

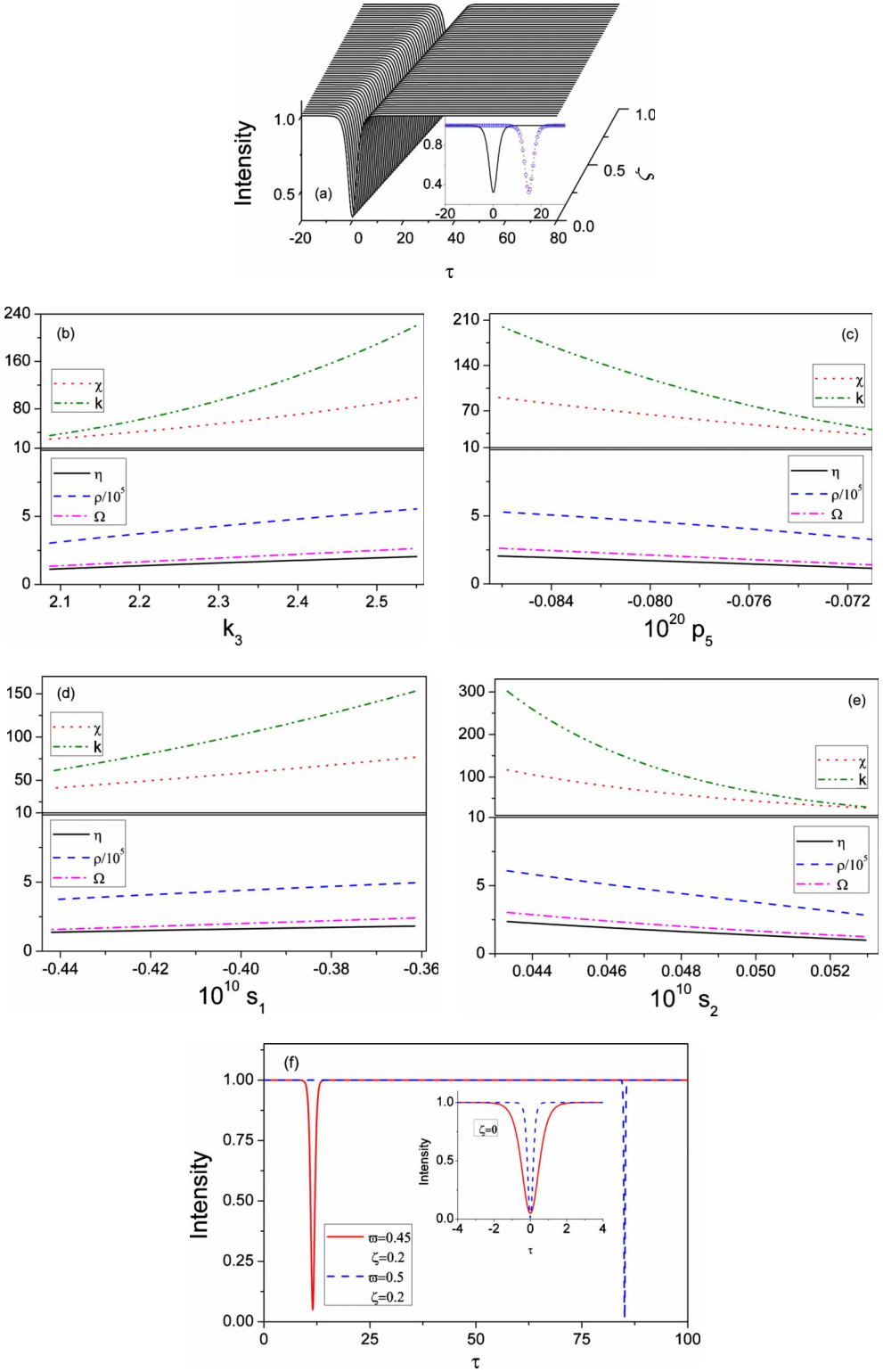


FIG. 4. (Color online) (a) The evolution of the gray solitary wave (12) for $\omega_m/\omega_p=0.9$, $\tilde{\omega}=0.42$; corresponding parameters are specified in the text. Numerical verification is shown in the inset. The influences of the higher-order effects (b) $k_3$, (c) $p_5$, (d) $s_1$, and (e) $s_2$ on $\chi$, $k$, $\eta$, and $\Omega$ of the gray solitary wave (12). (f) The distributions of the gray solitary wave (12) for $\omega_m/\omega_p=0.9$ when $\tilde{\omega}=0.45$, $\tilde{\omega}=0.5$. Here, $\lambda=10^5$ and soliton intensities are normalized as in Fig. 2.

eters, the gray solitary wave (12) possesses slightly different dip depths, obviously different widths, and remarkably different velocities, which are in agreement with the curves of Figs. 4(b)–4(e). These results show that $\chi^{(3)}$ nonlinearity, pseudo-$\chi^{(5)}$ nonlinearity, self-steepening, and second-order nonlinear dispersion mutually interact and reach a balance to ensure the formation of gray solitary waves; in particular, pseudo-$\chi^{(5)}$ nonlinearity and second-order nonlinear disper-

sion play a crucial role for the existence and properties of this case of gray solitary wave.

## IV. CONCLUSION

We have derived a higher-order NLS equation governing the propagation of few-cycle electromagnetic pulse in nonlinear NIMs under reasonable approximations. Using analytical method, we have presented three cases of exact gray solitary-wave solutions and the corresponding formation conditions in NIMs. According to the relation of parameters in NIMs with the Drude dispersion model, we have investigated the properties of these gray solitary waves under the influence of higher-order linear and nonlinear effects. Analytical and numerical results indicated that these exact gray solitary waves can exist in NIMs, and that the higher-order effects not only play an important role for the formation of gray solitary waves but also dominate their propagations in NIMs. The obtained results will be significant for the future studies on ultrashort solitons in the nonlinear NIMs.

## ACKNOWLEDGMENTS

This work was supported by the National Natural Science Foundation of China (Grants No. 60878008 and No. 60771052), the New Teacher Foundation of Ministry of Education of China (Grant No. 200801081014), and the Natural Science Foundation of Shanxi Province (Grant No. 2008012002-1).

[1] V. G. Veselago, Sov. Phys. Usp. **10**, 509 (1968).
[2] D. R. Smith, W. J. Padilla, D. C. Vier, S. C. Nemat-Nasser, and S. Schultz, Phys. Rev. Lett. **84**, 4184 (2000); R. A. Shelby, D. R. Smith, and S. Schultz, Science **292**, 77 (2001).
[3] J. B. Pendry, Phys. Rev. Lett. **85**, 3966 (2000).
[4] E. J. Reed, M. Soljacic, and J. D. Joannopoulos, Phys. Rev. Lett. **91**, 133901 (2003).
[5] A. A. Zharov, I. V. Shadrivov, and Yu. S. Kivshar, Phys. Rev. Lett. **91**, 037401 (2003).
[6] C. G. Parazzoli, R. B. Greegor, K. Li, B. E. C. Koltenbah, and M. Tanielian, Phys. Rev. Lett. **90**, 107401 (2003).
[7] C. M. Soukoulis, M. Kafesaki, and E. N. Economou, Adv. Mater. **18**, 1941 (2006).
[8] V. M. Shalaev, Nat. Photonics **1**, 41 (2007).
[9] J. Valentine, S. Zhang, T. Zentgraf, E. Ulin-Avila, D. A. Genov, G. Bartal, and X. Zhang, Nature (London) **455**, 376 (2008); J. Yao, Z. Liu, Y. Liu, Y. Wang, C. Sun, G. Bartal, A. Stacy, and X. Zhang, Science **321**, 930 (2008).
[10] A. K. Popov, V. V. Slabko, and V. M. Shalaev, Laser Phys. Lett. **3**, 293 (2006).
[11] A. K. Popov and V. M. Shalaev, Opt. Lett. **31**, 2169 (2006); N. M. Litchinitser and V. M. Shalaev, Nat. Photonics **3**, 75 (2009).
[12] S. C. Wen, Y. W. Wang, W. H. Su, Y. J. Xiang, X. Q. Fu, and D. Y. Fan, Phys. Rev. E **73**, 036617 (2006); Y. J. Xiang, S. C. Wen, X. Y. Dai, Z. X. Tang, W. H. Su, and D. Y. Fan, J. Opt. Soc. Am. B **24**, 3058 (2007).
[13] G. D'Aguanno, N. Mattiucci, M. Scalora, and M. J. Bloemer, Phys. Rev. Lett. **93**, 213902 (2004).
[14] A. D. Boardman, P. Egan, L. Velasco, and N. King, J. Opt. A, Pure Appl. Opt. **7**, S57 (2005); A. D. Boardman, R. C. Mitchell-Thomas, N. J. King, and Y. G. Rapoport, Opt. Commun. **283**, 1585 (2010).
[15] P. P. Banerjee and G. Nehmetallah, J. Opt. Soc. Am. B **24**, A69 (2007).
[16] N. A. Zharova, I. V. Shadrivov, A. A. Zharov, and Y. S. Kivshar, Opt. Express **13**, 1291 (2005).
[17] N. Lazarides and G. P. Tsironis, Phys. Rev. E **71**, 036614 (2005).
[18] M. Scalora, M. S. Syrchin, N. Akozbek, E. Y. Poliakov, G. D'Aguanno, N. Mattiucci, M. J. Bloemer, and A. M. Zheltikov, Phys. Rev. Lett. **95**, 013902 (2005); **95**, 239902(E) (2005).
[19] N. L. Tsitsas, N. Rompotis, I. Kourakis, P. G. Kevrekidis, and D. J. Frantzeskakis, Phys. Rev. E **79**, 037601 (2009).
[20] A. Joseph, K. Porsezian, and M. Wadati, J. Phys. Soc. Jpn. **78**, 044402 (2009).
[21] W. N. Cui, Y. Y. Zhu, H. X. Li, and S. M. Liu, Phys. Lett. A **374**, 380 (2009).
[22] P. Emplit, J. P. Hamaide, F. Reynaud, C. Froehly, and A. Barthelemy, Opt. Commun. **62**, 374 (1987).
[23] A. M. Weiner, J. P. Heritage, R. J. Hawkins, R. N. Thurston, E. M. Kirschner, D. E. Leaird, and W. J. Tomlinson, Phys. Rev. Lett. **61**, 2445 (1988).
[24] W. Zhao and E. Bourkoff, Opt. Lett. **14**, 703 (1989).
[25] Y. S. Kivshar, M. Haelterman, P. Emplit, and J.-P. Hamaide, Opt. Lett. **19**, 19 (1994).
[26] N.-C. Panoiu, D. Mihalache, and D.-M. Baboiu, Phys. Rev. A **52**, 4182 (1995).
[27] G. P. Agrawal, *Nonlinear Fiber Optics* (Academic, San Diego, 1995).
[28] R. Yang, R. Hao, L. Li, Z. Li, and G. Zhou, Opt. Commun. **242**, 285 (2004); R. Yang, R. Hao, L. Li, X. Shi, Z. Li, and G. Zhou, *ibid.* **253**, 177 (2005).
[29] L. D. Landau and E. M. Lifshitz, *Electrodynamics of Continuous Media* (Pergamon Press, New York, 1960).
[30] M. S. Syrchin, A. M. Zheltikov, and M. Scalora, Phys. Rev. A **69**, 053803 (2004).
[31] R. W. Ziolkowski and E. Heyman, Phys. Rev. E **64**, 056625 (2001); R. W. Ziolkowski and A. D. Kipple, *ibid.* **68**, 026615 (2003).
[32] G. Dolling, C. Enkrich, M. Wegener, C. M. Soukoulis, and S. Linden, Opt. Lett. **31**, 1800 (2006).
[33] T. Lepetit, É. Akmansoy, and J.-P. Ganne, Appl. Phys. Lett. **95**, 121101 (2009).
[34] Z. G. Dong, H. Liu, T. Li, Z. H. Zhu, S.-M. Wang, J. X. Cao, S. N. Zhu, and X. Zhang, Appl. Phys. Lett. **96**, 044104 (2010).
[35] I. Kourakis, N. Lazarides, and G. P. Tsironis, Phys. Rev. E **75**, 067601 (2007).